Mesostructured Hollow Spheres of Graphitic N-Doped Carbon Nanocast from Spherical Mesoporous Silica

Yongde Xia, Zhuxian Yang, and Robert Mokaya*

School of Chemistry, University of Nottingham, University Park, Nottingham NG7 2RD, United Kingdom

Received: August 26, 2004; In Final Form: September 24, 2004

Mesostructured hollow spheres of graphitic N-doped carbon (CNx) materials may be nanocast from solid core mesoporous silica SBA-15 spheres via a chemical vapor deposition (CVD) route. The hollow spheres are generated when the SBA-15 silica/carbon composite obtained after CVD is subjected to silica etching in hydrofluoric (HF) acid. Hollow spheres are only obtained for CVD temperatures above 900 °C; here we present data on materials prepared at 1000 °C. The use of acetonitrile as carbon precursor results in N-doped (CNx) materials with nitrogen content of ca. 6.5 wt %. The CNx hollow spheres prepared at 1000 °C exhibit a high level of graphitization as evidenced by powder X-ray diffraction analysis and Raman spectrocopic studies. The CNx hollow spheres also exhibit good mesostructural ordering and have high surface area (779 m^2/g) and pore volume (0.66 cm^3/g). We propose a mechanism for the formation of the hollow spheres and clarify the importance of the CVD temperature in their formation.

Introduction

Well-ordered mesoporous carbon materials are currently attracting intense interest due to their potential use as electrodes for energy storage, gas hosts, templates, or catalytic supports in fuel cells.[1−3] Among the synthesis routes used to obtain mesoporous carbons,[4] the solid template approach is attractive because it allows control of the pore structure and morphology of the resulting carbon materials. Solid templating is based on the pyrolysis of carbon precursors within the pore channels of silica or aluminosilicate templates, followed by the selective removal of the templates. During the past 5 years, much effort has been devoted to the synthesis of mesostructured carbon materials using mesoporous silica as solid templates.[5−13] A variety of mesoporous silicas including MCM-48,[5,6] SBA-15,[7−10] HMS,[11] MSU-H,[12] and MCM-41[13] have been used as hard templates to prepare ordered mesoporous carbon. In general, the structure of the resulting mesoporous carbon material is an inverse replica of the mesoporous silica template and the morphology of the silica template is retained in the carbon material.[7−12,14] Therefore, to fabricate mesoporous carbon materials of a particular morphology, it is necessary to control the morphology of the mesoporous silica templates.

The morphology of porous carbons is important with respect to their use in various applications. In particular, hollow sphere mesoporous carbon is desirable due to its low density, high surface area, and large pore volume. Carbon capsules composed of mesoporous shells with hollow cores have been synthesized using hierarchical silica spheres (with mesoporous shells and macroporous solid cores) as templates via a liquid impregnation method.[15] The carbon capsules, however, possessed a significant amount of microporosity (40% of pore volume), and the synthesis method involved several steps.[15] We have recently prepared micropore-free mesoporous carbon containing hollow spheres.[16] However not all the particles had a hollow sphere morphology.[16] Here we report on a synthesis route that utilizes spherical solid core mesoporous silica SBA-15 as a solid template and optimizes the morphology of the resulting mesoporous carbon toward hollow spheres. Furthermore, by using acetonitrile as the carbon source, N-doped mesoporous carbon (i.e., CNx) hollow spheres are obtained, which when prepared at suitably high chemical vapor deposition (CVD) temperature exhibit graphitization in their frameworks. The preparation of graphitic mesoporous carbon has only recently been achieved.[17−19] Ryoo and co-workers fabricated mesoporous carbons with graphitic frameworks via in situ conversion of aromatic compounds to mesophase pitch within the pores of mesoporous aluminosilicates.[17] Pinnavaia and co-workers have also reported on a similar synthesis method to graphitic mesoporous carbon using aromatic hydrocarbon as the carbon precursors via the replication of a mesostructured silica template on a catalyst.[18] We, on the other hand, have reported the synthesis of graphitic mesoporous carbon and nitrogen-doped carbon materials via a CVD method in which mesoporous SBA-15 was used as a solid template.[19] The synthesis of nitrogen-doped (CNx-type) mesoporous carbon materials has also been demonstrated by Schuth and co-workers, who used polyacrylonitrile as a carbon source.[9] This report presents a simple method for preparing well-ordered hollow spheres of mesoporous N-doped carbon (CNx) materials that also exhibit significant levels of graphitic character.

Experimental Section

Material Synthesis. Mesoporous silica SBA-15 solid core spheres were synthesized as follows:[20] Triblock copolymer P123 (3.0 g) and 0.5 g of cetyltrimethylammonium bromide were dissolved in a mixture containing 25 mL of ethanol, 30 mL of H_2O, and 60 mL of 2 N HCl, followed by addition of 10 mL of tetraethyl orthosilicate under stirring. After continuous stirring for 1 h at room temperature, the resulting gel was transferred to a Teflon-lined autoclave, which was first heated at 80 °C for 6 h, followed by further heating at 110 °C for 12 h. The autoclave was cooled to room temperature, and the solid product was obtained via filtration, air-dried, and calcined at 500 °C for 6 h under static air conditions to yield calcined SBA-15

* To whom correspondence should be addressed. E-mail: r.mokaya@nottingham.ac.uk.

10.1021/jp046142n CCC: $27.50
Published on Web 12/09/2004

spheres. The calcined SBA-15 spheres were used as a solid template for the preparation of mesoporous carbon as follows: An alumina boat with 0.5 g of SBA-15 was placed in a flow through tube furnace. The furnace was heated to the required temperature (900 or 1000 °C) under a nitrogen flow saturated with acetonitrile and then maintained at the target temperature for 3 h. The resulting SBA-15/carbon composites were washed with 10% hydrofluoric (HF) acid to remove the silica template. Finally the silica-etched carbon materials were dried in an oven at 120 °C overnight. The resulting N-doped (i.e., CNx) materials had a nitrogen content (wt %) of 6.6% and 6.4% for samples prepared at a CVD temperature of 900 and 1000 °C, respectively.

Material Characterization. Powder X-ray diffraction (XRD) analysis was performed using a Philips 1830 powder diffractometer with Cu Kα radiation (40 kV, 40 mA). Nitrogen sorption isotherms and textural properties of the materials were determined at −196 °C using nitrogen in a conventional volumetric technique by a Coulter SA3100 sorptometer. Before analysis, the samples were oven-dried at 150 °C and evacuated for 12 h at 200 °C under vacuum. The surface area was calculated using the Brunauer−Emmett−Teller (BET) method based on adsorption data in the partial pressure (P/P_0) range 0.05−0.2, and total pore volume was determined from the amount of the nitrogen adsorbed at P/P_0 = ca. 0.99. Elemental analysis was carried out using a CHNS analyzer (Fishons EA 1108). Scanning electron microscopy (SEM) images were recorded using a JEOL JSM-820 scanning electron microscope. Samples were mounted using a conductive carbon double-sided sticky tape. A thin (ca. 10 nm) coating of gold sputter was deposited onto the samples to reduce the effects of charging. Transmission electron microscopy (TEM) images were recorded on a JEOL 2000-FX electron microscope operating at 200 kV. Samples for analysis were prepared by spreading them on a holey carbon film supported on a grid. X-ray photoelectron spectroscopy (XPS) was carried out using the Kratos AXIS ULTRA with a monochromated Al Kα X-ray source (1486.6 eV) operated at 10 mA emission current and 15 kV anode potential. The analysis chamber pressure was better than 10^{-9} Torr. FAT (fixed analyzer transmission) mode was used, with pass energies of 160 eV (or 80 eV) for survey scans and 40 eV for high-resolution scans. The takeoff angle for the photoelectron analyzer was 90°, and the acceptance angle was 30° (in magnetic lens modes). Raman spectra were obtained on a Nicolet Almega Dispersive Raman microscope. The Raman spectra were collected by manually placing the probe tip near the desired point of the sample on a glass slide at room temperature.

Results and Discussion

The mesoporous silica SBA-15 template was prepared using a method that optimized the formation of spheres. This was confirmed by the SEM images shown in Figure 1. The SBA-15 template was made up of spheres (of size between 2 and 5 μm) as the only particle morphology (Figure 1). The spheres were mainly free-standing, but in some cases some aggregation was observed. The mesostructural ordering of the SBA-15 spheres was probed by nitrogen sorption analysis. The nitrogen sorption isotherm of the silica spheres is shown in Figure 2, and the corresponding textural properties are given in Table 1. The SBA-15 spheres exhibit a type IV isotherm with a typical capillary condensation step into uniform mesopores in the partial pressure (P/P_0) range 0.5−0.7. The silica spheres had a surface area of 1087 m^2/g and pore volume of 1.13 cm^3/g. The pore size was estimated to be ca. 6.0 nm. The sorption isotherm and textural properties confirm that the SBA-15 spheres possessed good mesostructural ordering and that they were suitable for use as solid templates for the nanocasting of mesostructured carbons.

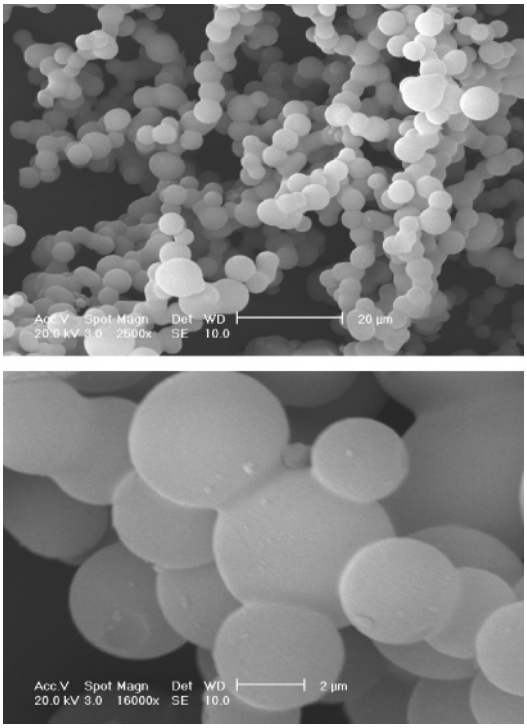

Figure 1. SEM images of mesoporous silica SBA-15 spheres used as a solid template.

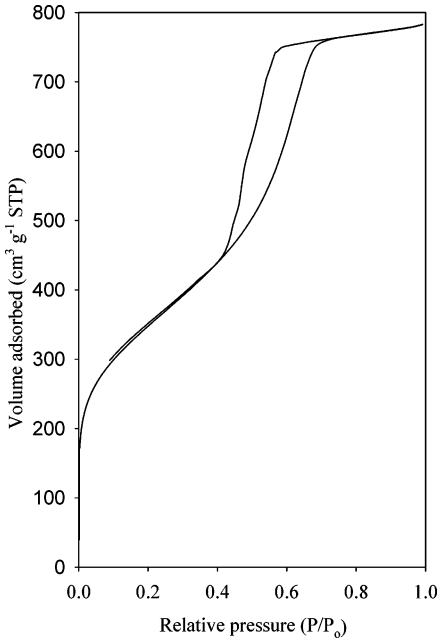

Figure 2. Nitrogen sorption isotherm of mesoporous silica SBA-15 spheres used as a solid template.

TABLE 1: Textural Properties and Elemental Composition of Graphitic N-Doped Carbon Materials Prepared via CVD with Acetonitrile as the Carbon Source

sample	CVD temp (°C)	N content (wt %)	surface area (m^2/g)	pore volume (cm^3/g)
silica (SBA-15)			1087	1.13
CNx	900	6.6	1019	0.83
CNx	1000	6.4	779	0.66

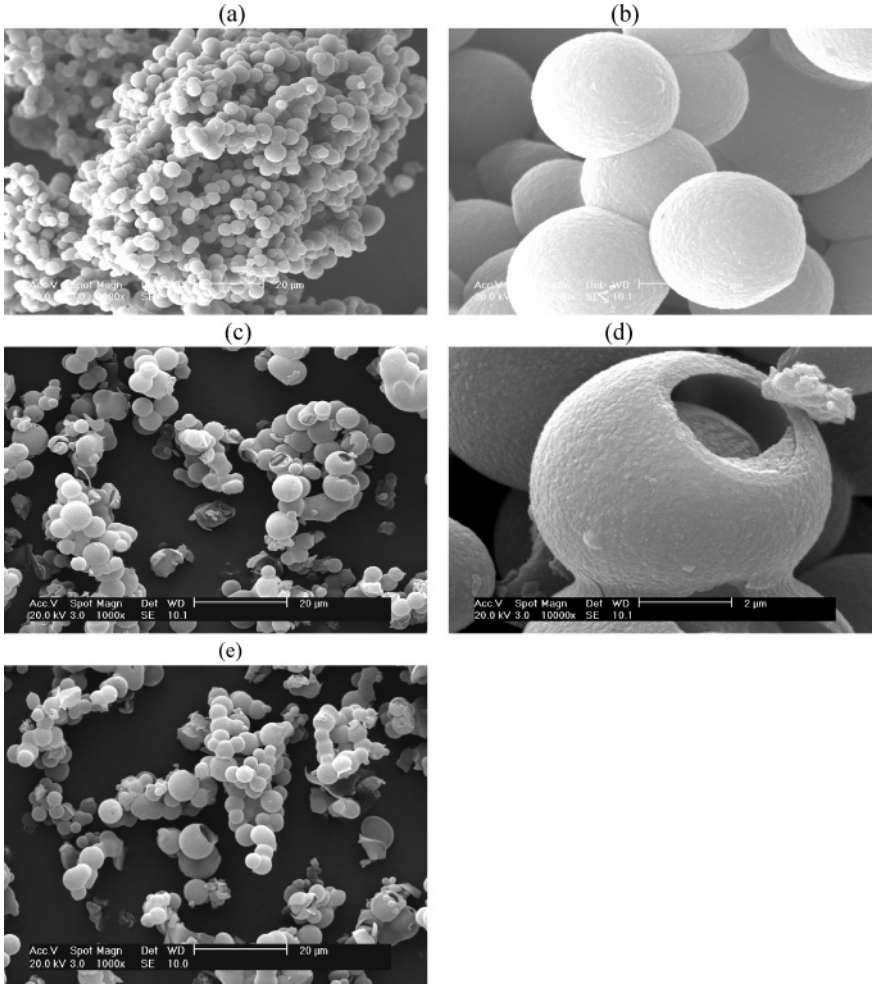

Figure 3. SEM images of (a,b) SBA-15/carbon composite prepared at a CVD temperature of 1000 °C before washing with HF acid and (c−e) silica-free mesoporous carbon after HF treatment.

Figure 3 shows the SEM images of the SBA-15/carbon composite obtained after chemical vapor deposition of acetonitrile into the silica spheres at 1000 °C and the silica-free carbon materials obtained after treatment in HF acid. The images clearly show that the spherical morphology and particle size of the SBA-15 template is replicated in the SBA-15/carbon composite (Figure 3a,b). Figure 3a shows that the composite is made up of spheres as the only particle morphology. At higher magnification (Figure 3b), it is possible to observe the well-formed silica/carbon spheres. On removing the silica, via etching in hydrofluoric (HF) acid, the resulting mesoporous N-containing carbon materials retain the spherical morphology with a particle size of between 3 and 5 μm as shown in Figure 3c−e. However, the spheres have hollow rather than solid cores as shown by some of the particles that are fractured to reveal hollow cores. Removal of the silica from the SBA-15/carbon composites by HF etching therefore results in the formation of hollow spheres with relatively thin outer shells. The hollow sphere morphology of the silica-etched carbon materials was also evidenced by the TEM images in Figure 4. The TEM images, which show well-formed spheres, are consistent with the formation of relatively thin (ca. 80 nm) shells with hollow interiors. The thickness of the shell appears to be relatively uniform throughout the particle.

To further confirm that the silica-free carbon spheres prepared at a CVD temperature of 1000 °C have hollow interiors, we subjected the spheres to compaction at 1.0 GPa for 1 h. To clarify the role that the silica etching step plays in the formation of hollow spheres, we also compacted the SBA-15/carbon composite. Figure 5a,b shows SEM images of the SBA-15/carbon composite and silica-free mesoporous carbon samples prepared at 1000 °C after compaction at 1.0 GPa for 1 h. The spheres of the compacted SBA-15/carbon composite are intact (Figure 5a), while the compacted silica-etched carbon material (Figure 5b) displays platelike particles resulting from crushed spheres. We did not observe any intact spheres for the compacted silica-free carbon samples. This provides further evidence that the carbon spheres are indeed hollow. We propose a mechanism (depicted in Scheme 1) for the formation of hollow carbon spheres from solid core spherical SBA-15. During the CVD process, the acetonitrile is first in contact with the surface

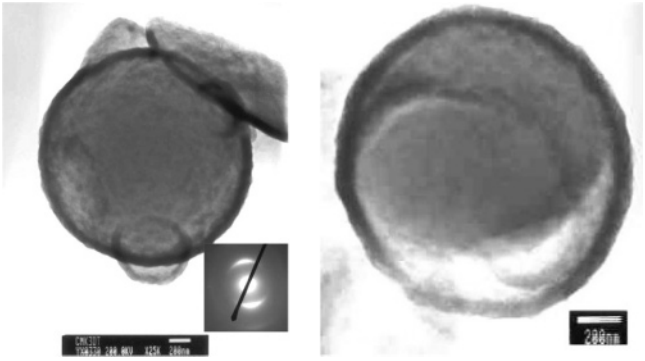

Figure 4. TEM images of hollow spheres of mesoporous carbon material prepared at a CVD temperature of 1000 °C. The inset is the corresponding SAED pattern.

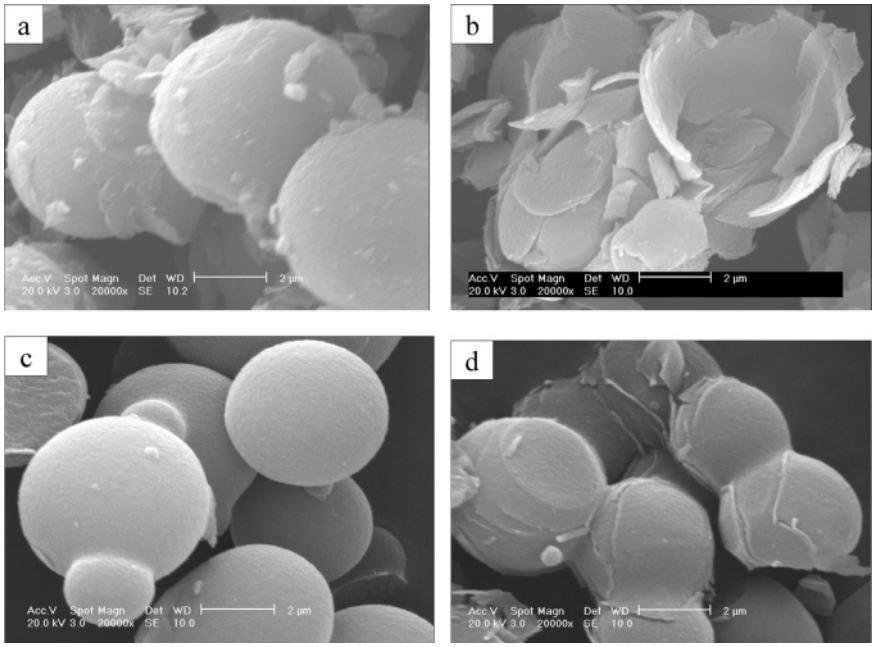

Figure 5. SEM images of mesoporous carbons prepared at a CVD temperature of 1000 °C (a,b) or 900 °C (c,d) after compaction at 1.0 GPa for 1 h; (a,c) SBA-15/carbon composites before HF treatment; (b,d) mesoporous carbon after HF treatment.

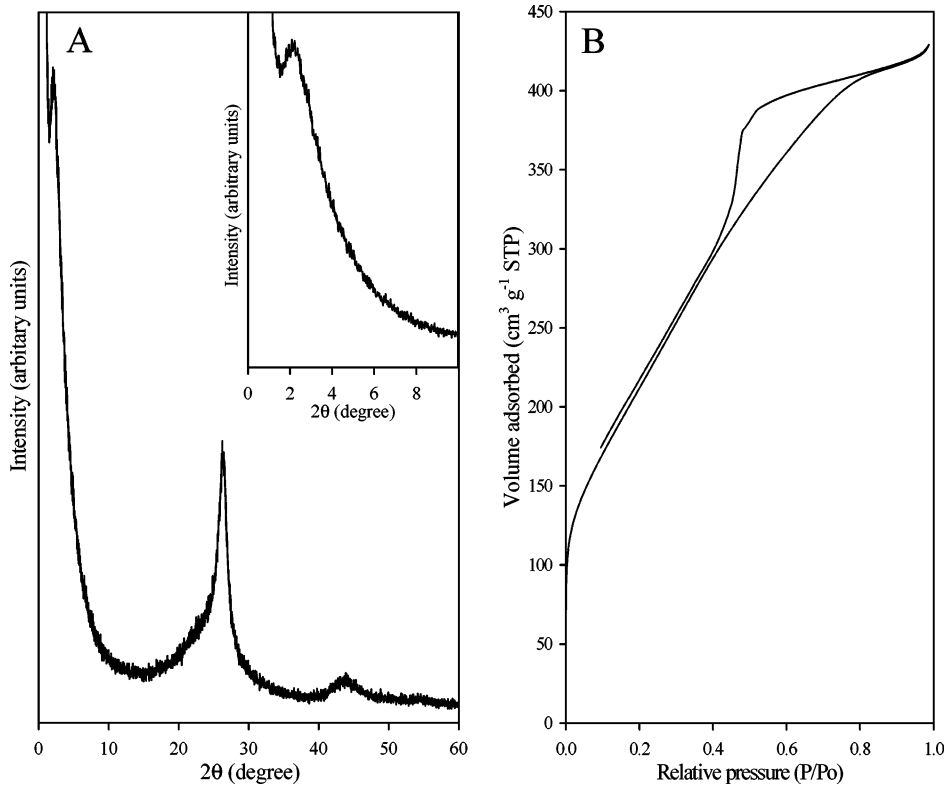

Figure 6. Powder XRD pattern (A) and nitrogen sorption isotherm (B) of hollow sphere mesoporous N-doped carbon prepared via CVD at 1000 °C. The inset in panel A is the enlarged XRD pattern at low angle for the hollow sphere mesoporous carbon material.

of SBA-15 spheres before diffusing into the interior of the silica. High CVD temperatures (e.g., 1000 °C) can accelerate carbonization of the acetonitrile once it is in contact with the surface/near-surface region of the spheres. The deposited carbon may block the pore channels and hinder access of acetonitrile to the core of the SBA-15 spheres. This would form a silica/carbon composite which is primarily composed of a carbon-filled silica outer shell surrounding a relatively purely siliceous inner core. Removal of the silica by HF acid results in a carbon shell with a hollow core.

SCHEME 1: Proposed Mechanism for the Formation of Mesoporous Carbon Hollow Spheres Nanocast from Solid Core Spherical Mesoporous Silica SBA-15

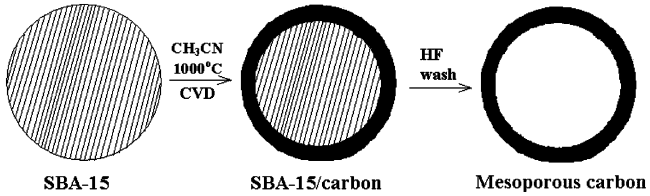

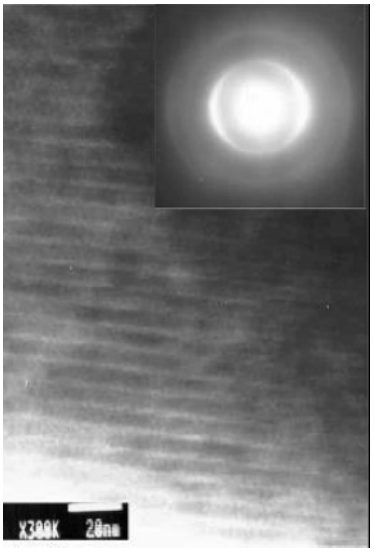

Figure 7. TEM image of a mesoporous N-doped carbon hollow sphere showing pore channel ordering. The inset is the corresponding SAED pattern.

The proposed mechanism implies that at lower CVD temperatures (e.g., 900 °C), carbonization would be slower (i.e., no pore blocking would occur) thus resulting in the infiltration of the acetonitrile carbon source into the interior of the solid template (SBA-15) silica spheres. This would ultimately result in the formation of solid core mesoporous carbon materials. This is indeed what is observed; to clarify the effect of CVD temperature on the formation of hollow carbon spheres, we subjected the silica/carbon composite and silica-etched carbon material prepared at 900 °C to compaction at 1.0 GPa for 1 h. The SEM images of the 900 °C SBA-15/carbon composite and silica-etched carbon sample after compaction at 1.0 GPa for 1 h are shown in Figure 5c,d. Both the composite and mesoporous carbon spheres are intact after compaction. The silica-free mesoporous carbon spheres, despite showing some fracture cracks on the surface, are not crushed (Figure 5d). This indicates that the spherical carbon material prepared at 900 °C has solid core spheres, which is consistent with our proposed mechanism. We confirmed using thermogravimetric analysis that the sample shown in Figure 5d did not contain any residual silica.

The structural and local ordering of the N-doped carbon hollow spheres prepared at 1000 °C was investigated by powder XRD and nitrogen sorption isotherms. The powder XRD pattern and sorption isotherm are shown in Figure 6. The powder XRD pattern shows a well-developed peak in the low 2θ region (insert of Figure 6A) at $2\theta = 2.11°$. We tentatively attribute this peak to the d_{200} diffraction from a hexagonal arrangement of pores in the carbon spheres. We are not able to observe the basal (100) peak due to limitations of our instrument. However, the presence of a peak in the low 2θ region indicates that the carbon spheres are structurally well ordered. The position of the peak implies a basal (d_{100}) spacing of ca. 8.4 nm and a unit cell parameter of 9.7 nm. The low 2θ peak suggests that the structural ordering of the SBA-15 template is replicated[5−7] in the carbon material. This is possible because the thickness of the carbon shells (ca. 80 nm) is sufficient to "copy" the pore structure of the SBA-15 silica template. We note that the thickness of the carbon shells is an indication of the extent to which the carbon source (acetonitrile) infiltrated the SBA-15 silica spheres. In addition to the low 2θ peak, the XRD pattern in Figure 6A exhibits a sharp peak at $2\theta = 26.2°$ and two further peaks at $2\theta = 43.4°$ and 54.6°. This peaks are (002), (101), and (004) diffraction peaks from graphitic carbon. The d_{002} spacing obtained from the (002) peak is 3.39 Å, which is very close to that of ideal graphite (with $d_{002} = 3.35$ Å). The hollow spherical mesoporous carbon material therefore possesses a significant level of graphitic character (crystallinity). We note in particular the relatively high intensity of the (002) peak as an indication of extensive graphitization in the N-doped carbon hollow spheres. The hollow sphere carbon material exhibits a type IV nitrogen sorption isotherm with a capillary condensation step into mesopores in the relative pressure (P/P_0) range 0.4−0.8 (Figure 6B). The isotherm is typical for well-ordered CMK-3 type mesoporous carbons.[7] The surface area and pore volume of the

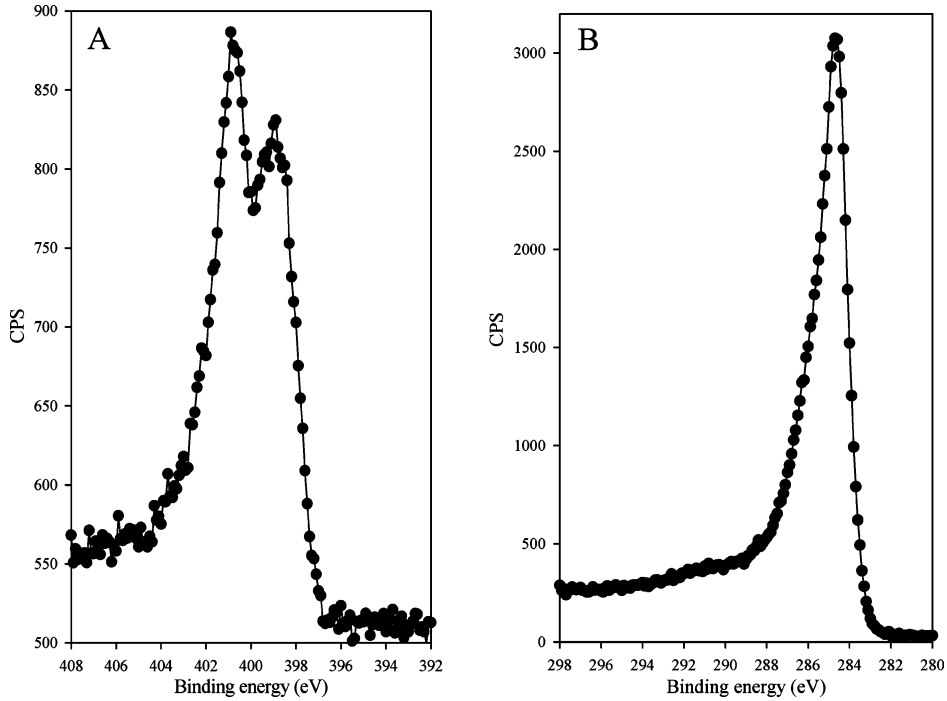

Figure 8. Enlarged N 1s (A) and C 1s (B) signals in the XPS spectra of mesoporous N-doped carbon hollow spheres prepared via CVD at 1000 °C with acetonitrile as the carbon source and SBA-15 as the template.

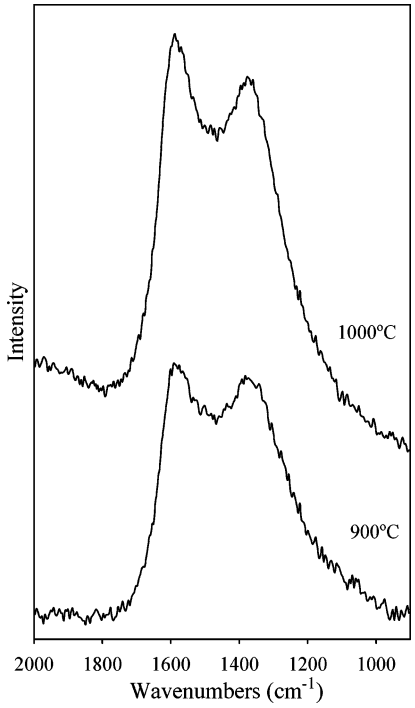

Figure 9. Raman spectra of hollow spheres of N-doped mesoporous carbon materials prepared via CVD with acetonitrile as the carbon source and SBA-15 as the template at 900 or 1000 °C.

mesoporous carbon are 779 m^2/g and 0.66 cm^3/g, respectively, with no contribution from micropores. The pore size, calculated using Barrett−Joyner−Halenda (BJH) analysis, is 4.7 nm.

The mesostructural ordering of the hollow spherical mesoporous carbon material was also evidenced by TEM as shown in Figure 7. Well-ordered arrays of the carbon "walls" and pore channels are clearly observed. From the TEM micrograph, it is possible to estimate that the hollow spherical mesoporous carbon possesses a diameter of ca. 5.0 nm, which is very close to the pore size obtained from nitrogen sorption. The selected area electron diffraction (SAED) patterns (insets of Figure 7 and Figure 4) show diffraction rings characteristic of graphitic ordering. The SAED patterns are in accordance with the XRD pattern (Figure 6A) and provide further evidence of graphitic character in the hollow spherical mesoporous N-doped carbon materials.

The binding between carbon and nitrogen in the N-doped mesoporous carbon spheres was probed by XPS. Figure 8 shows the XPS spectra of the sample prepared at 1000 °C. The spectra show a N 1s signal which was split into a high intensity peak at ca. 400.8 eV and a low intensity peak at 398.9 eV. These N 1s binding energies are consistent with the presence of highly coordinated (quaternary) nitrogen atoms (400.8 eV) and pyridine-like nitrogen atoms (398.9 eV) in graphitic sheets.[19,21] The C 1s peak for the mesoporous N-doped carbon spheres was observed at ca. 284.6 eV (consistent with sp^2 graphitic carbon) and displayed a slightly asymmetric nature. The Raman spectra shown in Figure 9 are also consistent with the presence of graphitic sheets within the pore walls of N-doped carbon materials. The Raman spectra, for materials prepared at a CVD temperature of 900 or 1000 °C, show two bands at ca. 1350 cm^{-1} (D band) and ca. 1580 cm^{-1} (G band). Band G is due to the carbon−carbon stretching (E_{2g}) mode for graphitic sheets.[22,23] The presence of this band therefore provides further evidence for the graphitic nature of the N-doped carbon spheres. We note that the intensity of band G is higher for the sample prepared at 1000 °C.

Conclusions

We have shown that hollow spheres of structurally well-ordered and graphitic mesoporous nitrogen-doped carbon may be nanocast using mesoporous silica SBA-15 solid core spheres as a template via a CVD route. The CVD temperature is an important consideration and should be higher than 900 °C and preferably 1000 °C for successful formation of carbon hollow spheres. The use of acetonitrile as a carbon precursor results in N-doped (CNx) materials with a nitrogen content of ca. 6.5 wt %. The CNx hollow spheres exhibit a high level of graphitization especially for materials prepared at a CVD temperature of 1000 °C. The CNx hollow spheres also exhibit good mesostructural ordering and have high surface area (779 m^2/g) and pore volume (0.66 cm^3/g). Mesoporous hollow spheres of graphitic CNx materials with well-ordered pore channels along with high surface area and pore volume are likely to find use in a variety of applications including gas storage, catalysis, or electrode materials.

Acknowledgment. The authors are grateful to the EPSRC for financial support.

References and Notes

(1) Dillon, A. C.; Jones, K. M.; Bekkedahl, T. A.; Kiang, C. H.; Bethune, D. S.; Heben, M. J. *Nature* **1997**, *386*, 377.

(2) Yang, Z.; Xia, Y.; Mokaya, R. *Adv. Mater.* **2004**, *16*, 727.

(3) Kang, M.; Yi, S. H.; Lee, H. I.; Yie, J. E.; Kim, J. M. *Chem. Commun.* **2002**, 1944.

(4) Kyotani, T. *Carbon* **2000**, *38*, 269.

(5) Lee, J.; Yoon, S.; Hyeon, T.; Oh, S. M.; Kim, K. B. *Chem. Commun.* **1999**, 2177.

(6) Ryoo, R.; Joo, S. H.; Jun, S. *J. Phys. Chem. B* **1999**, *103*, 7743.

(7) Jun, S.; Joo, S. H.; Ryoo, R.; Kruk, M.; Jaroniec, M.; Liu, Z.; Ohsuna, T.; Terasaki, O. *J. Am. Chem. Soc.* **2000**, *122*, 10712.

(8) Fuertes, A. B. *J. Mater. Chem.* **2003**, *13*, 3085.

(9) Lu, A.; Kiefer, A.; Schmidt, W.; Schueth, F. *Chem. Mater.* **2004**, *16*, 100.

(10) Alvarez, S.; Fuertes, A. B. *Carbon* **2004**, *42*, 433.

(11) Lee, J.; Yoon, S.; Oh, S. M.; Shin, C.-H.; Hyeon, T. *Adv. Mater.* **2000**, *12*, 359.

(12) Kim, S.-S.; Pinnavaia, T. J. *Chem. Commun.* **2001**, 2418.

(13) Tian, B.; Che, S.; Liu, Z.; Liu, X.; Fan, W.; Tatsumi, T.; Terasaki, O.; Zhao, D. *Chem. Commun.* **2003**, 2726.

(14) Yu, C.; Fan, J.; Tian, B.; Zhao, D.; Stucky, G. D. *Adv. Mater.* **2002**, *14*, 1742.

(15) Yoon, S. B.; Sohn, K.; Kim, J. Y.; Shin, C.-H.; Yu, J.-S.; Hyeon, T. *Adv. Mater.* **2002**, *14*, 19.

(16) Xia, Y.; Mokaya, R. *Adv. Mater.* **2004**, *16*, 886.

(17) Kim, T.-W.; Park, I.-S.; Ryoo, R. *Angew. Chem., Int. Ed.* **2003**, *42*, 4375.

(18) Kim, C. H.; Lee, D.-K.; Pinnavaia, T. J. *Langmuir* **2004**, *20*, 5157.

(19) Xia, Y.; Mokaya, R. *Adv. Mater.* **2004**, *16*, 1553.

(20) Zhao, D.; Sun, J.; Li, Q.; Stucky, G. D. *Chem. Mater.* **2000**, *12*, 275.

(21) (a) Sen, R.; Satishkumar, B. C.; Govindaraj, A.; Harikumar, K. R.; Renganathan, M. K.; Rao, C. N. R. *J. Mater. Chem.* **1997**, *7*, 2335. (b) Terrones, M.; Redlich, P.; Grobert, N.; Trasobares, S.; Hsu, W.-K.; Terrones, H.; Zhu, Y.-Q.; Hare, J. P.; Reeves, C. L.; Cheetham, A. K.; Ruhle, M.; Kroto, H. W.; Walton, D. R. M. *Adv. Mater.* **1999**, *11*, 655. (c) Xu, W.; Kyotani, T.; Pradhan, B. K.; Nakajima, T.; Tomita, A. *Adv. Mater.* **2003**, *15*, 1087. (d) Terrones, M.; Grobert, N.; Terrones, H. *Carbon* **2002**, *40*, 1665.

(22) Tuinstra, F.; Koenig, J. L. *J. Chem. Phys.* **1970**, *53*, 1126.

(23) Wilhelm, H.; Lelaurain, M.; McRae, E.; Humbert, B. *J. Appl. Phys.* **1998**, *84*, 6552.